INSTITUTE OF PHYSICS PUBLISHING PLASMA PHYSICS AND CONTROLLED FUSION

Plasma Phys. Control. Fusion **48** (2006) B39–B52 doi:10.1088/0741-3335/48/12B/S04

Progress on advanced tokamak and steady-state scenario development on DIII-D and NSTX

E J Doyle[1], A M Garofalo[2], C M Greenfield[3], S M Kaye[4], J E Menard[4], M Murakami[5], S A Sabbagh[2], M E Austin[6], R E Bell[4], K H Burrell[3], J R Ferron[3], D A Gates[4], R J Groebner[3], A W Hyatt[3], R J Jayakumar[7], J E Kinsey[8], B P LeBlanc[4], T C Luce[3], G R McKee[9], M Okabayashi[4], Y-K M Peng[5], C C Petty[3], P A Politzer[3], T L Rhodes[1], M R Wade[3], R E Waltz[3] and the DIII-D and NSTX Research Teams

[1] Department of Electrical Engineering and PSTI, University of California, Los Angeles, California 90095, USA
[2] Columbia University, New York, New York 10027, USA
[3] General Atomics, San Diego, California 92186-5608, USA
[4] Princeton Plasma Physics Laboratory, Princeton, New Jersey 08543-0451, USA
[5] Oak Ridge National Laboratory, Oak Ridge, Tennessee 37831, USA
[6] University of Texas-Austin, Austin, Texas 78712, USA
[7] Lawrence Livermore National Laboratory, Livermore, California 94550, USA
[8] Lehigh University, Bethlehem, Pennsylvania 18015, USA
[9] University of Wisconsin-Madison, Madison, Wisconsin 53706, USA

Received 23 June 2006
Published 8 November 2006
Online at stacks.iop.org/PPCF/48/B39

Abstract

Advanced tokamak (AT) research seeks to develop steady-state operating scenarios for ITER and other future devices from a demonstrated scientific basis. Normalized target parameters for steady-state operation on ITER are 100% non-inductive current operation with a bootstrap current fraction $f_{BS} \geqslant 60\%$, $q_{95} \sim 4$–5 and $G \equiv \beta_N H_{scaling}/q_{95}^2 \geqslant 0.3$. Progress in realizing such plasmas is considered in terms of the development of plasma control capabilities and scientific understanding, leading to improved AT performance. NSTX has demonstrated active resistive wall mode stabilization with low, ITER-relevant, rotation rates below the critical value required for passive stabilization. On DIII-D, experimental observations and GYRO simulations indicate that ion internal transport barrier (ITB) formation at rational-q surfaces is due to equilibrium zonal flows generating high local $E \times B$ shear levels. In addition, stability modelling for DIII-D indicates a path to operation at $\beta_N \geqslant 4$ with $q_{min} \geqslant 2$, using broad, hollow current profiles to increase the ideal wall stability limit. Both NSTX and DIII-D have optimized plasma performance and expanded AT operational limits. NSTX now has long-pulse, high performance discharges meeting the normalized targets for an spherical torus-based component test facility. DIII-D has developed sustained discharges combining high beta and ITBs, with performance approaching levels required for AT reactor concepts, e.g. $\beta_N = 4$, $H_{89} = 2.5$, with $f_{BS} > 60\%$. Most importantly, DIII-D

has developed ITER steady-state demonstration discharges, simultaneously meeting the targets for steady-state $Q \geqslant 5$ operation on ITER set out above, substantially increasing confidence in ITER meeting its steady-state performance objective.

1. Introduction

Steady-state operation would substantially enhance the attractiveness of the tokamak as a fusion power plant, by maximizing the operational duty factor and minimizing material fatigue from thermal and mechanical cycling. Such operation at $Q \geqslant 5$, where Q is the ratio of fusion power to input auxiliary power for heating and current drive, is one of two key ITER performance objectives [1]. Advanced tokamak (AT) research seeks to develop steady-state operating scenarios for ITER and other future devices from a demonstrated scientific basis. The AT concept was first developed in the early 1990s [2, 3], and demonstrating the feasibility of steady-state operation is sought through achieving appropriate normalized performance targets, as none of the current major tokamaks has a true steady-state capability. AT development is a major component of the DIII-D tokamak [4–8] and NSTX spherical torus (ST) [9–11] research programmes, as also on JT-60U [12] and JET [13]. This paper presents highlights of the significant progress made with regard to understanding, controlling and realizing AT plasmas on NSTX and DIII-D over the last two years, concentrating on core and global plasma conditions (i.e. edge and pedestal specific issues are not treated).

In the remainder of this paper, AT performance targets for steady-state operation and DIII-D and NSTX progress towards these targets are presented in the following sections. Recent improvements in plasma control capabilities for operation at high beta with tailored q-profiles, etc, are described in section 3, while progress on theory-based understanding of key aspects of AT plasma behaviour is presented in section 4. The significant recent progress in meeting normalized AT steady-state performance targets on DIII-D and NSTX is described in section 5. The paper concludes with a summary.

2. Performance targets for steady-state operation and DIII-D and NSTX progress relative to these targets

As compared with a conventional H-mode operation, fully non-inductive operation with no transformer-driven inductive plasma current ($f_{\mathrm{NI}} = 100\%$), requires a *simultaneous combination* of large self-driven bootstrap current fraction (f_{BS}) and high beta and confinement to maximize fusion power with reduced plasma current I_{p}. It is achieving these requirements simultaneously that forms the key challenge in AT research. A high bootstrap fraction is required in order to limit the auxiliary power required for current drive to economic levels. At a minimum, $f_{\mathrm{BS}} \geqslant 50\%$ is required, while $f_{\mathrm{BS}} \geqslant 60\%$ is highly desirable. Since $f_{\mathrm{BS}} \propto q\beta_{\mathrm{N}}$, this implies high q_{95} and q_{min}, from which it follows that AT plasmas operate at reduced plasma current compared with conventional H-mode. As fusion power maximizes at maximum I_{p}, there is therefore a conflict between the need to maximize f_{BS} and generate fusion power. As

$$Q \propto nT\tau \propto \left(\beta_{\mathrm{N}} \frac{IB_0}{a}\right)(H_{\mathrm{scaling}}\tau_{\mathrm{scaling}}), \tag{1}$$

where $\beta_{\mathrm{N}} \equiv \beta_{\mathrm{T}}/(I/aB_0)$ and $\beta_{\mathrm{T}} \equiv 2\mu_0\langle p\rangle/B_0^2$, the resolution to this conflict is to operate at significantly higher normalized beta, β_{N}, and higher normalized confinement, H_{scaling}, as

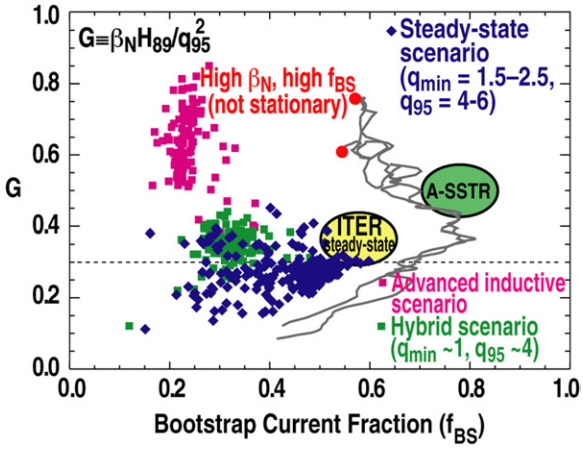

Figure 1. Global data for normalized fusion performance versus bootstrap current fraction in DIII-D, showing that steady-state demonstration plasmas are now meeting ITER normalized performance requirements. In addition, sustained DIII-D discharges, indicated by the grey traces, offer the prospect of higher, AT reactor relevant performance.

compared with conventional tokamaks. A convenient figure of merit for maximizing Q can be derived as [14]: $G \equiv \beta_N H_{scaling}/q_{95}^2$ [14]. In this paper, the confinement scaling used is that relative to L-mode, H_{89} [15].

DIII-D seeks to demonstrate the normalized performance targets required for steady-state operation on ITER, and explore operation at the higher performance levels required for steady-state reactor concepts. Approximate target parameters for ITER steady-state operation are [16]; $Q \geqslant 5$, corresponding to $G \geqslant 0.3$, with $f_{BS} \geqslant 60\%$, $f_{NI} = 100\%$, $q_{min} \geqslant 1.5$ and $q_{95} \sim 4$–5. As shown in figure 1, stationary, steady-state scenario plasmas on DIII-D are now *simultaneously* achieving both the performance (G) and bootstrap fraction (f_{BS}) targets for ITER, and as shown later also have $f_{NI} = 100\%$, substantially increasing confidence that ITER can operate in a steady-state regime. Also shown via the traces in figure 1 are sustained DIII-D discharges which offer the prospect of going substantially beyond minimum ITER requirements, with performance approaching that of AT reactor concepts such as the advanced SSTR [17].

NSTX seeks to demonstrate the normalized performance targets required for the proposed ST component test facility (ST-CTF) [18], with ITER relevance. The CTF is a proposed 8–12 MA machine with major radius $R = 1.2$ m, aspect ratio $A \geqslant 1.5$, and elongation $\kappa \leqslant 3$, with a goal of producing a neutron flux of (1–4) MW m^{-2} with $\beta_N = 4$–5, $\beta_T = 20$–30% and $f_{BS} \geqslant 50\%$ [17]. As can be seen in figure 2, NSTX plasmas obtained within the last two years have made very significant progress, and now demonstrate sustained ($\tau_{pulse}/\tau_E \sim 50$, where τ_{pulse} is the flattop discharge duration) high performance at the $\beta_N H_{89}$ product required for ST-CTF operation [18].

3. Improvements to plasma control capabilities for steady-state operation

A major difference between AT and conventional H-mode operation is that the former requires substantial active plasma control capabilities. The leading requirements are for (1) non-inductive current drive, to make up the difference between the bootstrap current and the total plasma current. Current drive on DIII-D is provided by neutral beams (NBCD), and

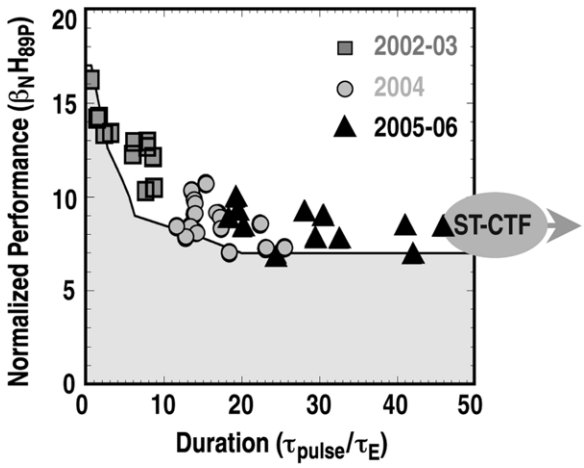

Figure 2. Global data for product of β_N and H_{89} versus flat-top duration normalized to energy confinement time on NSTX. Sustained plasma performance is now meeting targets for an ST-based CTF.

off-axis electron cyclotron current drive (ECCD) for current profile control [6], while NSTX has NBCD and high harmonic fast wave systems [9]. (2) Resistive wall mode (RWM) stabilization is required for operation substantially above the no-wall RWM beta limit. DIII-D has for several years employed both internal and external feedback control coils for RWM stabilization [7], while results from a new active RWM control system on NSTX [19], complementing previous passive stabilizer plates, are discussed below. Using rotational stabilization and error field minimization, both machines have demonstrated transient operation up to the ideal-wall limit, and sustained operation at over 50% above the no-wall limit. (3) Strong shaping (high elongation κ, and triangularity δ) to improve stability limits and confinement [20, 21].

Close fitting, passive plates on NSTX previously allowed stabilization of rotating plasmas at over 50% above the no-wall beta limit [22]. However, the addition of six new external active control coils has enabled the exploration of an important new ITER relevant regime, active RWM stabilization in plasmas with rotation rates ω_ϕ significantly below the critical value Ω_{crit} required for passive stabilization [19]. Shown in figure 3 are two NSTX plasmas, one with (solid curves) and one without (dashed curves) active RWM stabilization, and both initially operating at over 20% above the no-wall RWM limit. In the case of the discharge without active stabilization, $n = 3$ magnetic braking is applied (current shown in figure 3(c)), reducing the plasma rotation, figure 3(b), until an $n = 1$ RWM instability grows, figure 3(d), and the plasma disrupts. This discharge experimentally determines the critical toroidal rotation threshold Ω_{crit} for stabilization. By contrast, a second identical discharge, but with active RWM stabilization enabled (braking and stabilization coil current shown in figure 3(c)), persists for over 90 RWM growth times, as shown in figure 3(a), with rotation rates $\omega_\phi/\Omega_{crit}$ down to 0.2–0.3, i.e. with rotation substantially below the critical value for passive rotational stabilization, figure 3(b). This is a first such demonstration, and is ITER relevant as the rotation in that device may be substantially below Ω_{crit} [23]. The other major improvement on NSTX since 2004 is the implementation of new divertor poloidal field coils, providing enhanced plasma shaping capability, with the ability to run with $\kappa = 2.75$ and $\delta = 0.8$. The highest performance NSTX long pulse discharges shown in figure 2 took advantage of such improved shaping capability [11, 21].

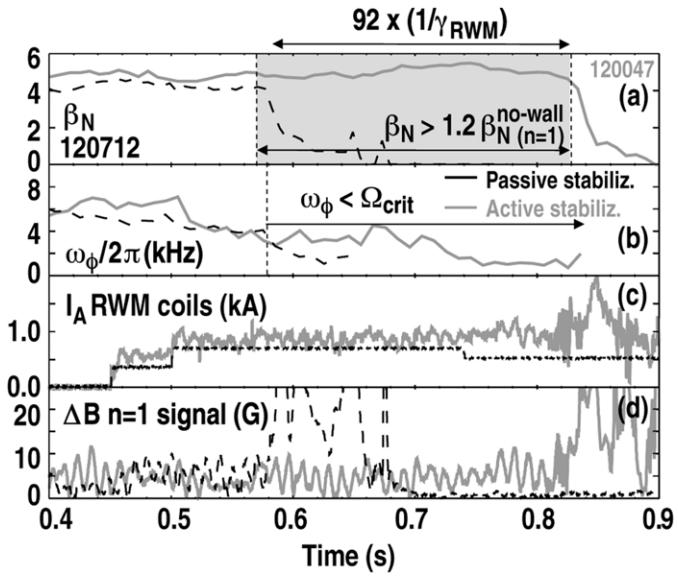

Figure 3. RWM feedback stabilization data from low rotation plasmas on NSTX. The solid curves are for a discharge with active RWM feedback, while the dashed curves are for a similar discharge, but without feedback stabilization. (*a*) β_N evolution, (*b*) plasma rotation frequency measured near $q = 2$, (*c*) current in external control coil, (*d*) $n = 1$ mode amplitude at the midplane. The discharge without active stabilization provides an experimental measurement of the critical rotation value required for passive stabilization. Both discharges have an $n = 3$ magnetic braking field applied to slow the plasma rotation, shown by the dc currents in (*c*).

In 2005, the active DIII-D RWM control system was improved to provide more robust stabilization in the presence of low rotation transients, such as occur during ELMs [7]. In the new approach, six external coils (C-coils) are feedback controlled on a slow time scale to maintain optimal error field correction, and hence maintain high average plasma rotation rates. At the same time, twelve internal coils (I-coils) are used to provide direct $n = 1$ RWM stabilization on a fast time scale, responding to modes destabilized during low-rotation transients. This improved RWM control system is key to sustaining the new DIII-D high beta, internal transport barrier (ITB) discharges discussed in section 5. In addition, several important improvements to DIII-D AT capabilities have been implemented during a shutdown for major machine upgrading which lasted from April 2005 to April 2006. The most important of these changes is that two of seven neutral beams have been reversed (rotated in toroidal injection angle), so as to provide a new simultaneous co-/counter-NBI capability, which is now operational on DIII-D. A second major improvement is a new high triangularity pumped lower divertor. Previously, the lower pumped divertor was low triangularity, $\delta \sim 0.3$, while now both upper and lower divertors can pump plasmas with $\delta \sim 0.6$–0.8, at $\kappa \sim 2.0$.

4. Advances in plasma understanding

Understanding of plasma rotation and momentum transport is, in general, not as developed as that for ion thermal transport, but plasma rotation is key to both plasma confinement quality (via rotation effects on $E \times B$ shearing rates), and RWM stabilization, as described above. However in recent NSTX experiments [24], quantitative agreement has been found between

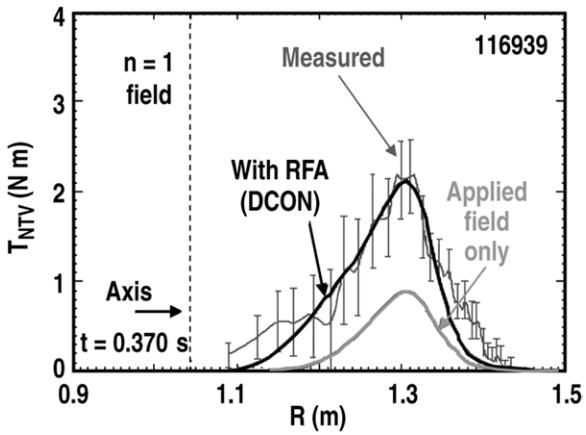

Figure 4. Comparison of measured and calculated rotational drag torques from an applied $n = 1$ non-axisymmetric field on NSTX. The calculations use the NTV theory, and are in excellent quantitative agreement with the measurements when resonant field amplification effects are included.

measurements of rotation damping and the theory of neoclassical toroidal viscosity (NTV) [25], when the effect of toroidally trapped particles is included, while similar DIII-D experiments are ongoing [26]. In the NSTX experiment, the same set of external coils used for RWM control (described above) was used to apply $n = 1$–3 non-axisymmetric magnetic field perturbations. The dissipation of the plasma toroidal angular momentum in response to this applied field was observed (magnetic braking) and compared with calculations of the expected drag torque, based on NTV theory. As can be seen from figure 4, for an $n = 1$ applied field there is excellent agreement between the measurements and theory, when resonant field amplification effects are taken into account. This result suggests that NTV theory, including the effect of toroidal-trapped particles and non-cylindrical geometry, is a viable model for torque balance in a tokamak.

On DIII-D, an improved understanding of how to access high β_N simultaneously with ITB operation to improve confinement has emerged from a series of closely coupled experiments and stability modelling runs [7]. This modelling is similar to and builds on the original AT modelling of Turnbull *et al* [3], but with a more peaked pressure profile and less strongly reversed q-profile (and RWM stabilization for operation above the no-wall limit). The modelling was performed for a fixed pressure profile with $P(0)/\langle P\rangle \sim 3$, and a range of q-profiles with varying q_{min}, as shown in figure 5(*a*). The resulting calculated $n = 1$ kink, no-wall and ideal-wall stability limits are shown in figure 5(*b*), from which it can be seen that the ideal-wall limit increases significantly for $q_{min} \geqslant 2$, indicating a potential region of operation with $\beta_N \geqslant 4$ (above the no-wall limit, using RWM stabilization). The reason for the increase in the ideal-wall limit is the improved wall coupling of the kink mode with the broad, hollow current profiles used in the modelling. The broad, weakly reversed q-profile is also favourable for the creation of moderate ITBs (i.e. ITBs with moderate profile gradients) at large radius, which is reflected in the pressure profile used. Thus, the modelling suggests a path to simultaneous improvements in both beta and confinement, by operation at $q_{min} \geqslant 2$ with broad, weakly reversed q-profiles.

With regard to ITBs, a major step forward in understanding ITB triggering under ITER relevant conditions has been made on DIII-D. On JET and many other devices, ITB operation is usually accessed via triggering at rational q-values [27], i.e. there is a lower power threshold

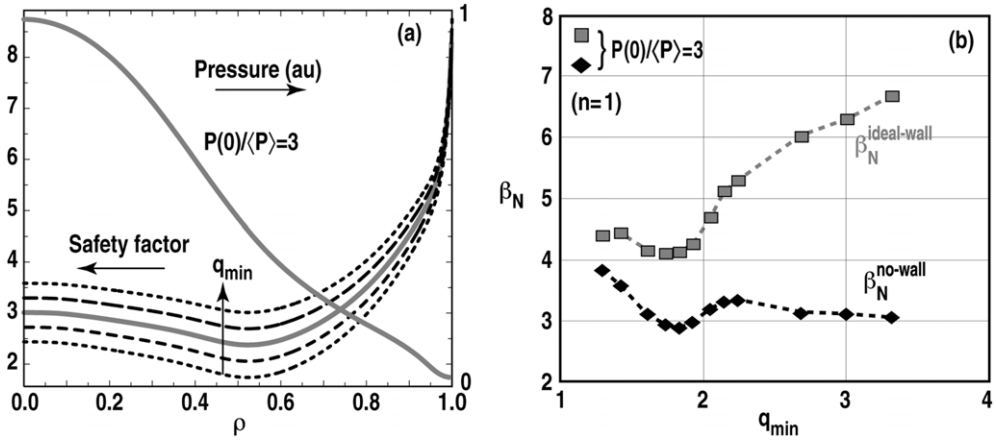

Figure 5. (*a*) Input q and pressure profiles for stability modelling. The variation in $q_{\min}$ used in the modelling is indicated by the dashed lines, while the pressure profile is consistent with the presence of moderate ITBs. (*b*) Results of stability modelling of $n = 1$ kink instabilities as a function of $q_{\min}$, for the profiles shown in (*a*). It is apparent that the ideal wall beta limit increases substantially for $q_{\min} \geqslant 2$, opening a path to high beta operation with RWM stabilization.

for ITB formation at low order rational q-values. This is critical for ITB access on JET, and potentially on ITER, since these machines have a relatively low power density. On DIII-D, a combination of detailed experimental measurements of ITBs, triggered just prior to a $q = 2$ surface entering plasmas with reversed q-profiles and L-mode edges [28], combined with nonlinear simulations using the GYRO gyrokinetic code (including electron dynamics) [29], has led to the development of a new model for this effect. In this model, the ITB formation is due to persistent, non-zero time average 'profile corrugations' in the radial electric field E_r and the temperature profiles, created by $n = 0$ zonal flow structures stemming from the low density of rational surfaces in the vicinity of low-order rational-q values. As shown in figure 6, the GYRO simulations indicate a large, persistent E_r structure just inside rational low order q-values ($q = 2$ in this case), with very large local $E \times B$ shear levels. This strong local $E \times B$ shear is sufficient to modify the local temperature profiles, triggering ITB formation. This picture is supported by turbulence measurements, including the observation of local shear formation in the poloidal turbulence velocity, figure 7(*a*), coinciding with a reduction in turbulence amplitude, figure 7(*b*), and ITB formation, figure 7(*c*).

5. High normalized performance discharges on DIII-D and NSTX

By utilizing the improvements in plasma control capability and understanding described in the previous sections, plasma performance has been significantly improved in terms of meeting AT performance goals on both NSTX and DIII-D. Three examples are considered, one from NSTX, and two from DIII-D. On NSTX, the plasma shaping improvements described earlier, combined with passive and active RWM stabilization, have led to a significant extension in plasma duration at high performance. Such a discharge is illustrated in figure 8, where the discharge duration is $\tau_{\text{pulse}}/\tau_E \sim 50$, where $\tau_E \sim 30$ ms, or $\tau_{\text{pulse}}/\tau_{\text{R}} \sim 5$, where $\tau_{\text{R}} \sim 300$ ms is the current relaxation (or redistribution) time. As can be seen from figure 8(*b*), β_{N} is maintained in a range 4–6 for ∼1 s, where 6 is the ideal-wall limit, with a maximum β_{T} of 17%, while $H_{89} \sim 2$. This discharge maintains the ST-CTF performance target of $\beta_{\text{N}} H_{89} \geqslant 10$

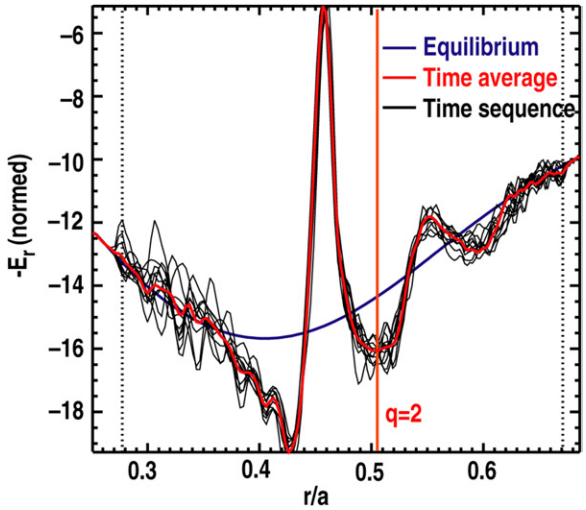

Figure 6. Nonlinear GYRO simulations for DIII-D discharge 121727, showing normalized input equilibrium E_r profile (blue), time sequence profiles showing zonal flow induced E_r (black curves), and time average E_r due to the zonal flows (red). Note that the zonal flows have a non-zero E_r time average in the vicinity of the $q = 2$ rational surface, generating large $E \times B$ shear levels.

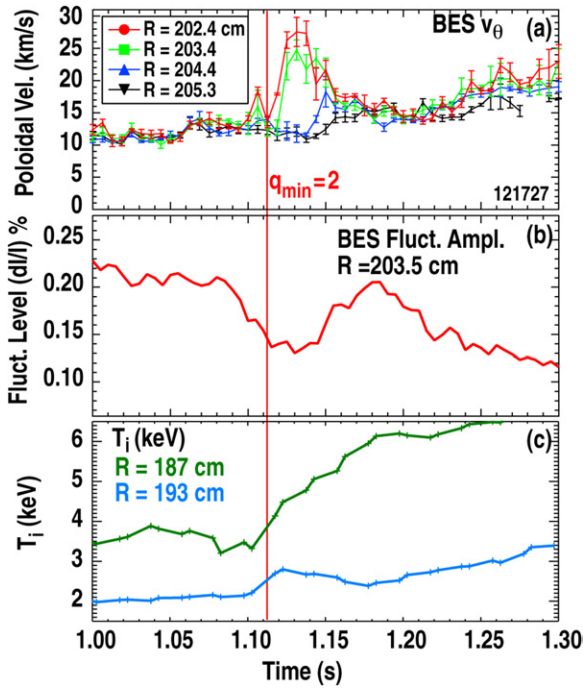

Figure 7. Experimental DIII-D data for the same discharge as simulated in figure 7, showing: (*a*) formation of strong shear in the poloidal flow velocity as the $q = 2$ surface enters the plasma, (*b*) reduced density fluctuation levels and (*c*) two core T_i channels indicating ITB formation at the time of the $q = 2$ crossing.

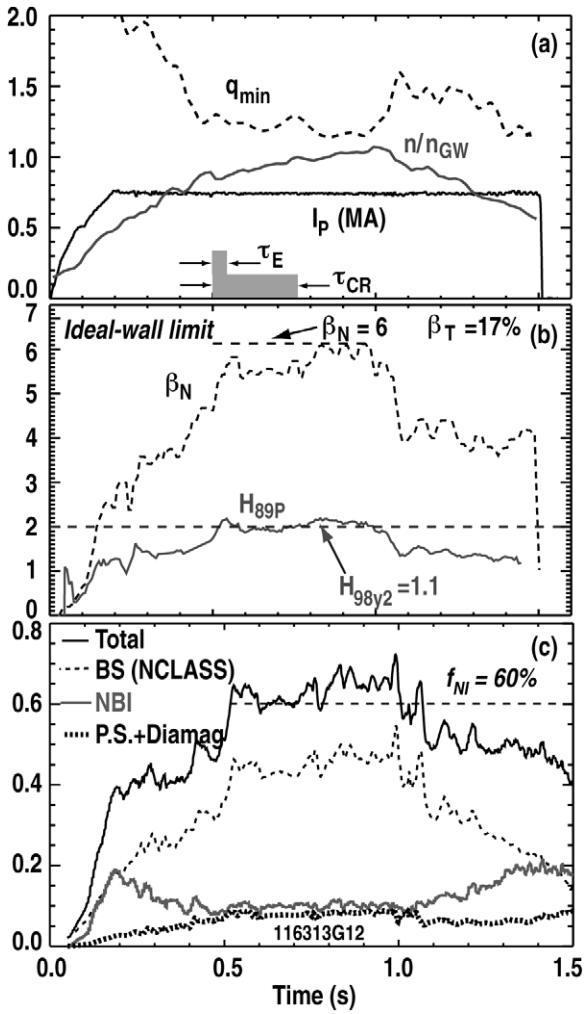

Figure 8. Time evolution of NSTX long pulse, high performance discharge 116313, showing (*a*) I_p, density normalized to the Greenwald density, and q_{min}, (*b*) β_N, H_{89}, (*c*) current fractions inferred from TRANSP analysis, showing $f_{NI} \geqslant 60\%$. Note that the MSE determined q_{min} remains above 1 throughout.

for ∼0.5 s. It should also be noted that $q_{min} > 1$ is maintained throughout the discharge, evaluated using MSE data (see figure 8(*a*)). Analysis indicates that redistribution of fast-ions by core MHD activity plays an important role in maintaining elevated $q_{min} > 1$ late in the discharge [11, 30]. TRANSP transport analysis [31] of this discharge (figure 8(*c*)) shows $f_{NI} \geqslant 60\%$, with f_{BS} of up to 50%, again meeting ST-CTF targets. Plasma profiles and transport rates are shown in figure 9. As can be seen, electron thermal transport is the dominant loss channel on NSTX, while ion thermal transport is at neoclassical values across much of the plasma radius, consistent with the presence of an ITB in the ion channel. The achievement of sustained, long pulse, high performance discharges such as this opens a path to AT research on NSTX, and substantially increases confidence in an ST-CTF meeting its design objectives.

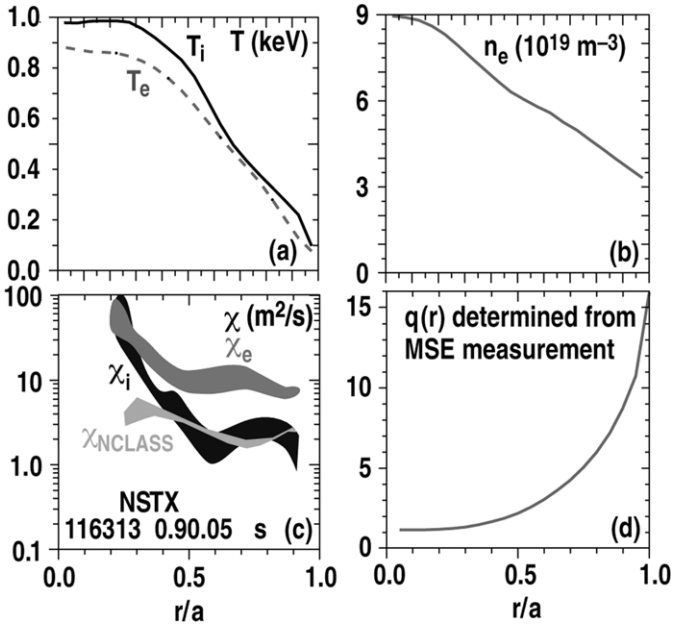

Figure 9. Plasma profiles and transport analysis for the NSTX discharge shown in figure 8. (*a*) T_e and T_i, (*b*) density profile, (*c*) electron and ion thermal diffusivities and ion neoclassical transport level, (*d*) MSE determined q-profile.

On DIII-D, sustained discharges have been created with $\beta_N = 4$ maintained for 2 s [7], as shown in figure 10. These plasmas operate at ∼50% above the no-wall beta limit (well represented by $4\,l_i$ on DIII-D), using the improved RWM stabilization system described in section 2. As can be seen from the plasma profiles shown for a similar discharge in figure 11, these plasmas have a broad, weakly reversed q-profile, with apparent ITBs in the ion temperature, density and rotation profiles, but not in the electron temperature profile. TRANSP transport analysis (figure 12) confirms the presence of an ITB in the ion, but not in the electron thermal channel. Gyrokinetic analysis using the GKS code [32] indicates that the measured $E \times B$ shearing rate is comparable to or exceeds the calculated turbulence growth rates across much of the plasma radius, and that ITG is the dominant turbulence mode in this plasma. It should be noted that discharges with ITBs were previously typically limited to operation at $\beta_N < 3$ by plasma stability limits [33], so these discharges represent a major advance in combining high beta with high confinement. Specifically, these plasmas are a realization of the route to high beta indicated by the stability modelling presented in section 4, using combined I_p and B_T ramps to create the desired conditions of $q_{min} \geqslant 2$ with broad, weakly reversed q-profiles. Plasma performance in these plasmas substantially exceeds that required for ITER steady-state targets, but at present is non-stationary due to the use of the I_p and B_T ramps. Creating a future stationary version of these discharges will require increased off-axis ECCD to maintain the hollow current profile created by the B_T ramp.

The main highlight of DIII-D progress on AT scenario development over the last two years is the realization of discharges with fully relaxed current profiles which *simultaneously meet all the ITER steady-state normalized performance targets* [8]. An example of such a fully integrated discharge is shown in figure 13, with ITER normalized target performance levels indicated. These steady-state demonstration discharges do not contain ITBs but have ion thermal transport rates moderately above neoclassical over much of the plasma radius.

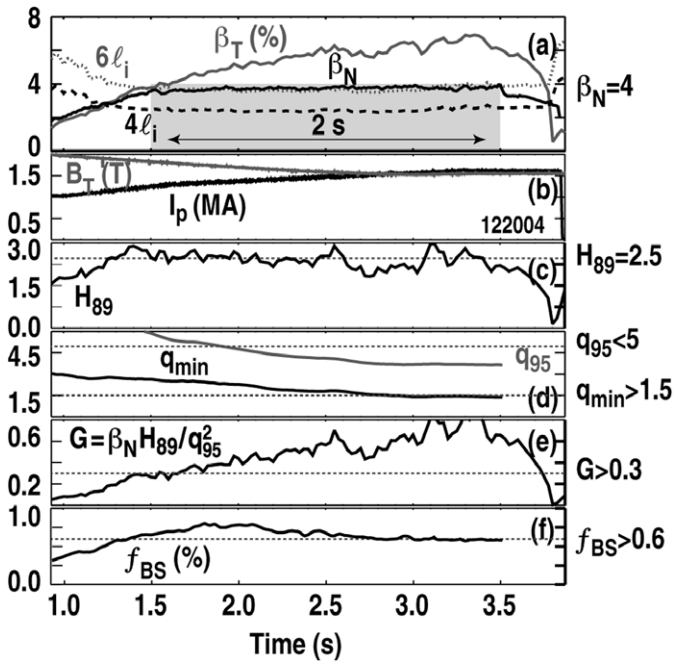

Figure 10. Time evolution of DIII-D discharge 122004 with sustained $\beta_N = 4$ for ~2 s. (*a*) β_N and β_T. Also shown are 4 and 6 times the internal inductance l_i. On DIII-D, $4l_i$ is a good indicator of the no-wall beta limit, (*b*) I_p and B_T, which are ramping during the discharge, i.e. the discharge has sustained high performance, but is non-stationary. (*c*) H_{89}, (*d*) q_{95} and q_{min}, (*e*) normalized fusion performance, G and (*f*) bootstrap current fraction. Normalized ITER steady-state plasma target parameters are indicated by horizontal dashed lines in (*c*)–(*f*).

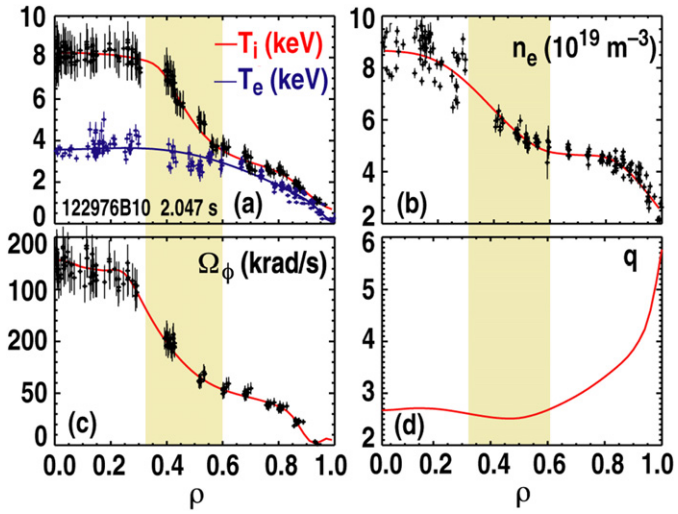

Figure 11. Plasma profiles for DIII-D discharge 122976 at 2.05 s, showing: (*a*) T_e and T_i, (*b*) density profile, (*c*) toroidal rotation profile and (*d*) q-profile. ITBs are apparent in the $T_i n_e$ and rotation profiles, but not T_e.

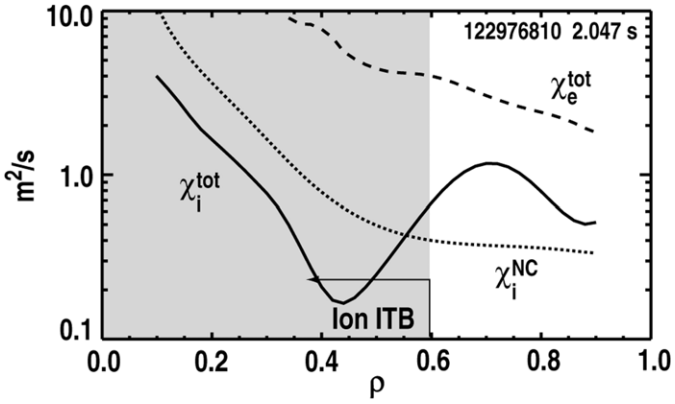

Figure 12. Transport analysis for the same discharge illustrated in figure 11, indicating the presence of an ITB in the ion thermal transport channel inside $\rho \sim 0.6$, and that there is no ITB in the electron channel.

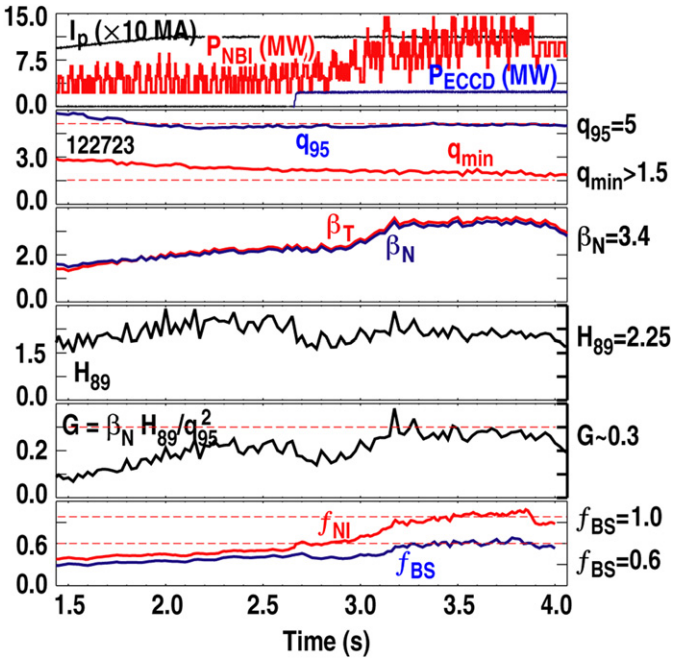

Figure 13. Time evolution of DIII-D discharge 122723, which simultaneously meets all ITER steady-state normalized performance targets. (*a*) I_p, NBI and ECCD power, (*b*) q_{95} and q_{min}, (*c*) β_N and β_T, (*d*) H_{89}, (*e*) normalized fusion performance, G and (*f*) non-inductive and bootstrap current fractions. Normalized ITER steady-state plasma target parameters are indicated by horizontal dashed lines in (*b*)–(*f*).

Inductive and total current profiles determined from analysis of a series of equilibrium reconstructions for this discharge (figure 14) confirm 100% non-inductive operation, with a relaxed current profile in which the inductive Ohmic current contribution is both globally and locally ~0. While these plasmas do not fully conform to reactor conditions (e.g. they operate with $T_i > T_e$), the realization of these ITER demonstration discharges substantially increases confidence in obtaining steady-state operation with $Q \geqslant 5$.

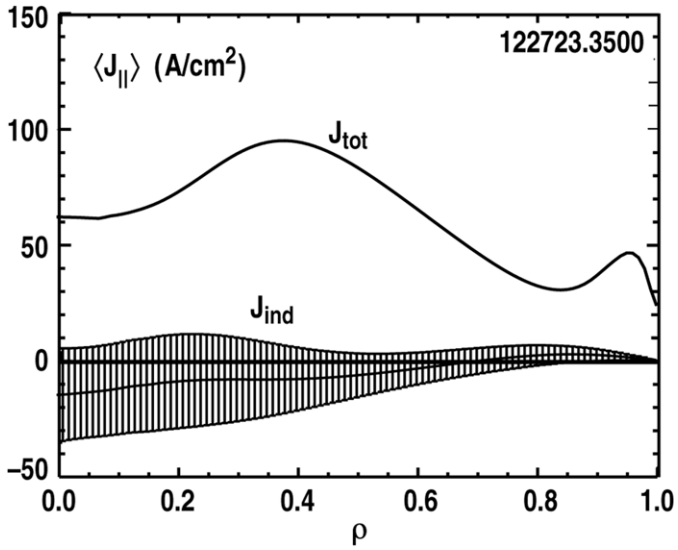

Figure 14. Inductive and total current profiles determined from analysis of a series of equilibrium reconstructions for discharge 122723, at 3.5 s. The Ohmic inductive current is both globally and locally ∼0.

6. Summary

In summary, both NSTX and DIII-D have made substantial progress in the development of AT scenarios over the last two years. Highlights for the two machines are as follows.

For DIII-D: (1) development of ITER steady-state demonstration discharges, simultaneously meeting normalized performance targets for steady-state $Q \geqslant 5$ operation on ITER; and (2) development of sustained, but non-stationary discharges combining high beta and ITBs, demonstrating performance levels required for AT reactor concepts.

For NSTX: (1) sustained normalized performance at levels required for an ST-based CTF, opening a path to AT research in the ST configuration; and (2) demonstration of active RWM stabilization at ITER-relevant low rotation rates, below the critical value required for passive rotational stabilization.

Acknowledgments

This work was supported by the US Department of Energy under DE-FG03-01ER54615, DE-FG02-89ER53297, DE-FC02-04ER54698, DE-FG02-95ER54303, DE-AC02-76CH03073, DE-AC05-00OR22725, DE-FG03-97ER54415, W-7405-ENG-48, DE-FG02-92ER54141 and DE-FG03-96ER54373.

References

[1] ITER Physics Basis 1999 *Nucl. Fusion* **39** 2137
[2] Taylor T S 1994 *et al Plasma Phys. Control. Fusion* **36** B229
[3] Turnbull A D *et al* 1995 *Phys. Rev. Lett.* **74** 718
[4] Wade M R *et al* 2003 *Nucl. Fusion* **43** 634
[5] Greenfield C M *et al* 2004 *Plasma Phys. Control. Fusion* **46** B213

[6] Luce T C for the DIII-D Team 2005 *Nucl. Fusion* **45** S86
[7] Garofalo A M *et al* 2006 *Phys. Plasmas* **13** 056110
[8] Murakami M *et al* 2006 *Phys. Plasmas* **13** 056106
[9] Kaye S M *et al* 2005 *Nucl. Fusion* **45** S168
[10] Kessel C E *et al* 2006 *Phys. Plasmas* **13** 056108
[11] Menard J E *et al* 2006 *Proc. 33rd EPS Conf. on Plasma Physics (Rome, Italy)* O2.002
[12] Ide S and the JT-60 Team 2005 *Nucl. Fusion* **45** S48
[13] Tuccillo A A *et al* 2006 *Nucl. Fusion* **46** 214
[14] Luce T C 2005 *Fusion Sci. Technol.* **48** 1212
[15] Yushmanov P N 1999 *et al Nucl. Fusion* **30**
[16] Polevoi A R *et al* 2005 *Nucl. Fusion* **45** 1451
[17] Kikuchi M, Seki Y and Nakagawa K 2000 *Fusion Eng. Des.* **48** 265
[18] Peng Y-K M *et al* 2005 *Plasma Phys. Control. Fusion* **47** B263
[19] Sabbagh S A *et al* 2006 *Phys. Rev. Lett.* **97** 045004
[20] Ferron J R *et al* 2005 *Phys. Plasmas* **12** 056126
[21] Gates D A *et al* 2006 *Phys. Plasmas* **13** 056122
[22] Sabbagh S A *et al* 2006 *Nucl. Fusion* **46** 635
[23] Liu Y *et al* 2005 *Nucl. Fusion* **45** 1131
[24] Zhu W *et al* 2006 *Phys. Rev. Lett.* **96** 225002
[25] Shaing K C *et al* 1986 *Phys. Fluids* **29** 521
[26] Jackson G L *et al* 2006 *Proc. 33rd EPS Conf. on Plasma Physics (Rome, Italy)* P5.143
[27] Joffrin E *et al* 2003 *Nucl. Fusion* **43** 1167
[28] Austin M E 2006 *et al Phys. Plasmas* **13** 082502
[29] Waltz R E *et al* 2006 *Phys. Plasmas* **13** 052301
[30] Menard J E *et al* 2006 *Phys. Rev. Lett.* **97** 095002
[31] Hawryluk R J 1980 *Proc. Course in Physics Close to Thermonuclear Conditions (Varenna, 1979)* vol 1 (Brussels: CEC) p 19
[32] Waltz R E *et al* 1999 *Phys. Plasmas* **6** 4265
[33] Wolf R C 2003 *Plasma Phys. Control. Fusion* **45** R1